

Technical Paper by K.R. Reddy, S. Kosgi and E.S. Motan

INTERFACE SHEAR BEHAVIOR OF LANDFILL COMPOSITE LINER SYSTEMS: A FINITE ELEMENT ANALYSIS

ABSTRACT: The use of various types of geosynthetics to construct landfill composite liner systems results in interfaces between different geosynthetics, and between geosynthetics and compacted cohesive soil liners/subgrade soil. These interfaces are potentially critical for stability due to their in-plane shear behavior. Conventional limit equilibrium analyses can provide an overall assessment of composite liner system stability; however, they lack the capability to compute displacements along the critical shear plane, and the resulting strain levels within the composite liner systems. In this study, the shear displacements of typical landfill composite liner system interfaces in response to municipal solid waste loads were evaluated using a finite element analysis. The interface shear-displacement parameters determined from available laboratory direct shear test data were used for the analysis. A parametric study was performed for soft, intermediate and stiff municipal solid waste conditions to evaluate the effect of different types of municipal solid waste on composite liner behavior.

KEYWORDS: Landfill, Composite liner system, Geosynthetics, Interface shear, Finite element analysis.

AUTHORS: K.R. Reddy, Assistant Professor, and S. Kosgi, Graduate Research Assistant, Department of Civil and Materials Engineering, University of Illinois at Chicago, 2095 Engineering Research Facility, 842 West Taylor Street, Chicago, Illinois 60607, USA, Telephone: 1/312-996-4755, Telefax: 1/312-996-2426; and E.S. Motan, Senior Geotechnical Engineer, RUST Environment & Infrastructure, 1240 East Diehl Road, Naperville, Illinois 60563, USA, Telephone: 1/708-955-6628, Telefax: 1/708-955-6601.

PUBLICATION: *Geosynthetics International* is published by the Industrial Fabrics Association International, 345 Cedar St., Suite 800, St. Paul, Minnesota 55101, USA, Telephone: 1/612-222-2508, Telefax: 1/612-222-8215. *Geosynthetics International* is registered under ISSN 1072-6349.

DATES: Original manuscript received 7 November 1995, revised version received 1 April 1996 and accepted 3 April 1996. Discussion open until 1 November 1996.

REFERENCE: Reddy, K.R., Kosgi, S. and Motan, S., 1996, "Interface Shear Behavior of Landfill Composite Liner Systems: A Finite Element Analysis", *Geosynthetics International*, Vol. 3, No. 2, pp. 247-275.

1 INTRODUCTION

Various types of landfill composite liner systems have been developed to prevent leachate migration into the subsurface environment. Typically, these composite liners consist of a compacted clay layer overlain by a geomembrane and other geosynthetic components such as geotextiles and geonets. Under certain conditions, geosynthetic clay liners are also used as a substitute for clay liners. The static and seismic stability of the base and side slopes of composite liners is a major concern due to the low shear resistance of various interfaces within these systems. With the possible exception of situations in which a marginally adequate subsoil is present beneath the composite liner, failure of the municipal solid waste (MSW) mass due to in-plane shear within the composite liner is typically considered to be the determining factor for stability assessments. Therefore, landfill stability analyses very often include potential failure planes which are, or, are at least partially located along the base and side slopes of composite liners. The use of smooth geomembranes almost certainly ensures that the critical stability plane includes a portion of the interface between the smooth geomembrane and another geosynthetic or compacted cohesive soil liner/subgrade soil.

Limit equilibrium slope stability analyses are commonly used to evaluate the factor of safety of the MSW mass along critical interfaces within composite liners based on the ratio of the resisting forces to driving forces along the critical stability planes (Duncan 1992; Mitchell and Mitchell 1992). These analyses assume that the MSW and the composite liner interfaces develop their limiting strength at the same time and to the same extent at all points along the critical plane. Such an approach lacks the capability to incorporate differences in the stress-strain behavior of different materials and interfaces involved in the overall stability. Many existing federal and state solid waste regulations do not specifically require analyses more involved than limit equilibrium methods.

Several stability analysis methods capable of incorporating stress-strain behavior exist as alternatives to limit equilibrium methods (Duncan 1992). These methods do not directly yield a factor of safety; however, they lead to a better understanding of the incremental behavior of different materials and their interfaces as the system approaches a state of failure. Also, the effects of nonlinearity in material properties can be easily evaluated by such techniques.

This paper reports the results of a research project that was initiated in 1994 at the University of Illinois at Chicago to evaluate landfill composite liner deformations and stresses in response to incremental loading of MSW. A nonlinear finite element code capable of representing interface shear behavior was used to analyze the response of the MSW and the composite liner. The cell geometry included a flat base composite liner section and a side slope composite liner. The MSW was assumed to be placed in horizontal increments on the base composite liner as well as on the side slope composite liner. A MSW face slope of 1 vertical:3 horizontal (1V:3H) was maintained on the cell interior.

The stress-strain characteristics of the composite liner interfaces were obtained from laboratory test data which was available to the writers. The stress-strain behavior of the MSW was approximated using properties of a highly organic soil. The finite element analysis methodology, along with the procedures to calculate the input parameters for the interfaces and the MSW, are described in detail. The results, which include induced

shear stresses and displacements within typical composite liners, are discussed. Finally, conclusions and recommendations for designing stable landfill composite liner systems are presented.

2 CHARACTERISTICS OF LANDFILL COMPOSITE LINER SYSTEM INTERFACES

2.1 Introduction

There are several interfaces along which slip may occur in a landfill composite liner system. These include interfaces between technically acceptable combinations of geotextiles, geonets, geomembranes, drainage geocomposites, geosynthetic clay liners and soil. The determination of interface shear stress/shear displacement behavior and shear strength parameters, namely adhesion and the friction angle between interface materials, is essential for an accurate assessment of the composite liner interface stability. It is necessary to evaluate the interface shearing resistances of specific combinations of geomembranes, geotextiles, geonets and compacted clay liner materials in order to identify the critical interface conditions that can lead to failure of the composite liner.

Laboratory direct shear (ASTM D 5321) and pullout tests are often used to determine the interface strength parameters for different geosynthetic composite liner components. Less frequently, ring shear tests have also been performed to determine the interface shear strength parameters. These different test methods are described in detail by Kosgi and Reddy (1995). The shear strength parameters are defined according to the Mohr-Coulomb failure criterion:

$$\tau_p = c_l + \sigma_n \tan \delta_l \quad (1)$$

where: τ_p = interface shear strength between two materials; σ_n = effective normal stress on the shear plane; c_l = adhesion between the interface materials, and δ_l = interface friction angle of geosynthetic composite liner components.

Until recently, little information was available concerning interface shear strength values for various geosynthetic combinations used in composite liners. Following the failure of a hazardous waste landfill unit at Kettleman Hills in California, landfill designers began to study interface shear strengths in more detail (Seed et al. 1990; Mitchell et al. 1990; Byrne et al. 1992). The interface shear strength values between various geosynthetics and soils, and between geosynthetic components have been reported by Koerner (1994), Sharma and Lewis (1994), Seed et al. (1990) and Martin et al. (1984). These authors reported that: (i) the friction angle between cohesionless soils and geomembrane materials (17° to 27°) is less than the internal friction angle of the cohesionless soils (30° to 50°); (ii) the interface friction angles between geomembranes and geotextiles are quite variable (6° to 28°) depending on the type of materials; and (iii) the sand to geotextile interface friction angles (23° to 30°) are less variable and generally higher than the other combinations tested. The large variation in the reported interface shear strength values was attributed to variations in testing procedures, normal stress, soils and geosynthetics. The range of values represent both peak and residual interface friction angle values.

The published interface shear strength and interface friction angle values provide a general range of values, but the values chosen for final design should ideally be based on a testing program using site specific soils and project specific geosynthetics. For the purpose of this study, the following two types of landfill composite liner interfaces were considered:

- (1) A composite liner that includes components exhibiting low interface shear strength values. Typical examples of such interfaces arise from the use of drainage geocomposites (a geonet with heat-bonded layers of nonwoven geotextile on both sides) placed directly on a smooth geomembrane, or a smooth geomembrane placed directly on a compacted cohesive soil liner.
- (2) A composite liner essentially the same as the above with the exception that a textured geomembrane replaces the smooth geomembrane.

The focus of this paper is the behavior of the geomembrane-nonwoven geotextile interface for both smooth and textured high density polyethylene (HDPE) geomembranes. The interface shear stress/shear displacement parameters used in the analyses were obtained using a large-scale (0.3 m × 0.3 m) direct shear apparatus. The direct shear test results are shown in Figure 1. Using the data shown in Figure 1, the peak shear strength parameters c_I and δ_I were evaluated. The c_I and δ_I values for the smooth geomembrane-geotextile interface were 1.4 kPa and 11° , respectively. For the textured geomembrane-geotextile interface, $c_I = 12$ kPa and $\delta_I = 30^\circ$.

2.2 Modeling of Interface Shear Stress/Shear Displacement Behavior of Landfill Composite Liner Interfaces

For the finite element analysis, the interface shear stress/shear displacement behavior of the composite liner interfaces must be accurately modeled. A simple model to describe the shear behavior of an interface involves using a hyperbolic relationship between the shear stress and the relative shear displacement at the interface (Clough and Duncan 1969). This hyperbolic relationship describes the nonlinear, stress dependent, interface shear stress/relative shear displacement relationship at an interface. The hyperbolic formulation is given by:

$$\tau = K_{st} \delta_s \quad (2)$$

where: τ = shear stress; δ_s = average relative shear displacement; and K_{st} = tangent shear stiffness. The value of K_{st} for loading conditions is given by:

$$K_{st} = K_s \gamma_w \left(\frac{\sigma_n}{P_a} \right)^n \left(1 - \frac{R_f \tau}{\tau_f} \right)^2 \quad (3)$$

where: K_s = dimensionless shear coefficient; n (modulus exponent) and R_f (failure ratio) = experimentally determined constants; γ_w = unit weight of water; P_a = atmospheric pressure; τ_f = shear stress at failure; and σ_n and τ = normal stress and shear stress acting on the interface, respectively.

The K_{st} value for unloading-reloading conditions is expressed as:

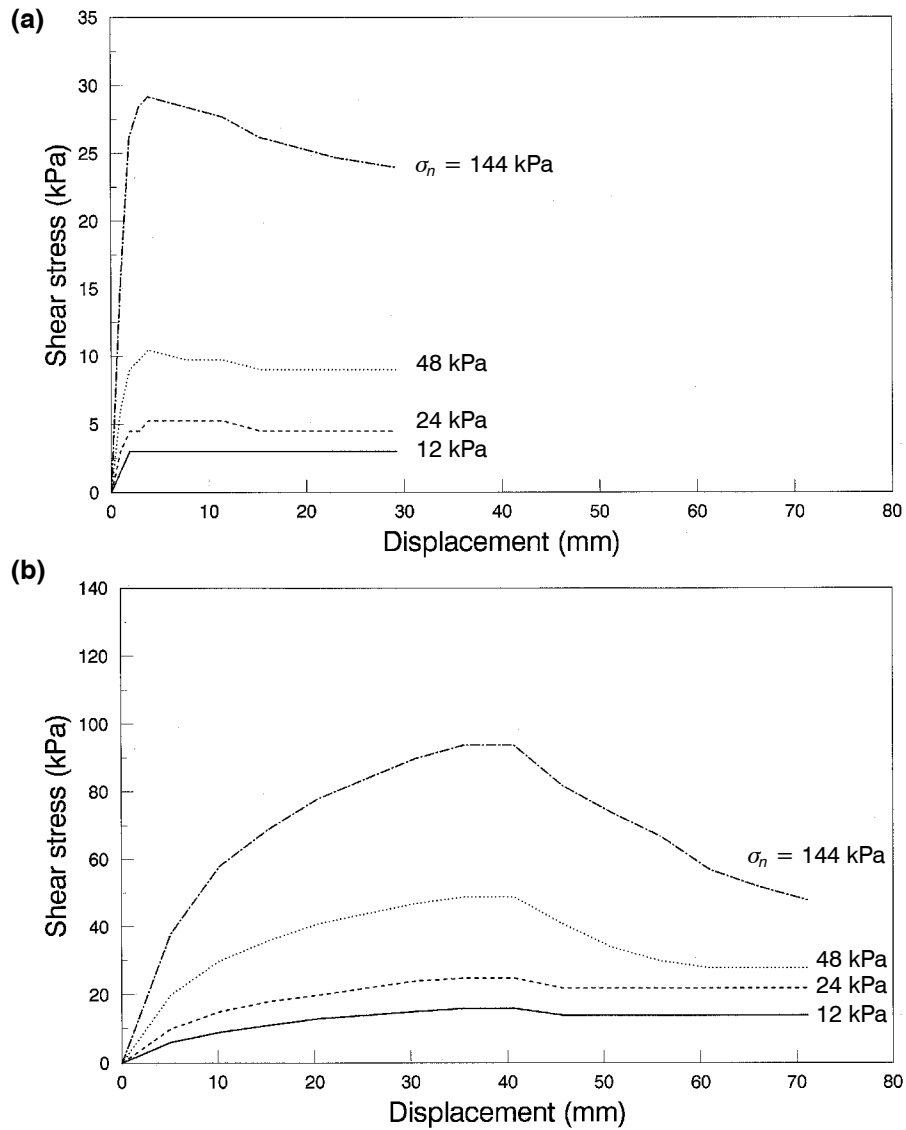


Figure 1. Interface direct shear test results for: (a) smooth HDPE geomembrane-nonwoven geotextile; (b) textured HDPE geomembrane-nonwoven geotextile.

Note: σ_n = effective normal stress.

$$K_{st} = K_{lur} \gamma_w \left(\frac{\sigma_n}{P_a} \right)^n \quad (4)$$

where K_{lur} is a dimensionless unloading-reloading shear coefficient.

Interface shear stress/shear displacement can be represented by a hyperbolic formulation provided that the parameters K_s , K_{ur} , n and R_f are known. The procedures to determine these parameters for the two interfaces (smooth and textured HDPE geomembrane-nonwoven geotextiles) are described in Section 4.2.

3 CHARACTERISTICS OF MSW

Relatively little is known about the geotechnical engineering properties of MSW. These properties depend on the composition of the solid waste in a typical MSW landfill which varies significantly with location and economic conditions of the localities served by the disposal facility. Landfill operation practices such as, MSW lift thickness and the MSW compaction achieved, can also affect the MSW behavior. Due to the presence of many large-scale constituents within the landfill MSW, there are difficulties in credible sampling and testing of this material. This difficulty is further compounded by the fact that MSW composition and properties are likely to vary erratically within a landfill and are also likely to change with time due to decomposition.

3.1 Unit Weight of MSW

The unit weight of MSW varies depending on the initial composition, compactive effort, decomposition, settlement and moisture content. The unit weight for MSW reported in the literature varies from 3.14 to 13.2 kN/m³ (Sharma and Lewis 1994). For the purpose of this study, a unit weight of 10.2 kN/m³ was assumed for the MSW. The moisture content of MSW also varies with its initial condition, local climatic conditions, landfill operating procedures (e.g. type of daily cover used), the effectiveness of the leachate collection and removal system if one exists, and the amount of moisture removed with landfill gas. Typical moisture content values reported in the literature for MSW range from 15 to 40% (Tchobanoglous et al. 1993).

3.2 Shear Strength of MSW

The Mohr-Coulomb failure criterion is generally used to represent the shear strength of MSW and is expressed as:

$$\tau = c_r + \sigma_n \tan \phi_r \quad (5)$$

where: τ = shear strength along a given plane; c_r = cohesion; σ_n = effective stress normal to the plane; and ϕ_r = internal friction angle. Field and laboratory test data for the shear strength parameters of MSW is limited. Existing information indicates a wide range of internal friction angles and cohesion values from various tests. To estimate the shear strength of the MSW in landfills, the general approaches used are: (i) laboratory testing; (ii) back calculation from field tests and operational records; and (iii) in situ testing.

Fang et al. (1977) used the double punch test for determining the tensile resistance of compacted MSW. Values of $c_r = 63$ kPa and $\phi_r = 19^\circ$ were estimated using the double punch test and the unconfined compression test methods. Landva and Clark (1990) reported values of c_r and ϕ_r ranging from 0 to 23 kPa and 24 to 41°, respectively, based

on drained direct shear tests on specimens measuring 287 mm × 434 mm. Siegel et al. (1990) reported direct shear tests on 106 mm diameter specimens of mixed MSW and inferred from these tests that internal friction angles varied from 39° to 81°. Poran and Ali (1989) used unconsolidated-undrained triaxial tests to determine the strength of partially saturated incinerated MSW residue and reported apparent internal friction angles of 43° to 45° at a maximum dry density of 13.5 kN/m³ and an optimum moisture content of 23.5% (60-70% saturation).

Attempts to evaluate the in situ shear strength of the landfill MSW have only been partially successful (Landva and Clark 1990; Singh and Murphy 1990). Much more work is required to develop a rational methodology to separate the frictional and cohesive components of the MSW if the use of the Mohr-Coulomb shear strength criterion is continued. Singh and Murphy (1990) present recommended strength properties for MSW based on a summary of the results from a series of in situ experiments.

3.3 Stress-Strain Behavior of MSW

Stability analysis methods which are based on limit equilibrium methods require input of the shear strength parameters, c and ϕ . For soils, these shear strength parameters correspond to the response of the soil at strain levels usually not exceeding 15 to 20%. The stress-strain response of MSW has not been investigated because of difficulties in sampling and testing representative MSW in landfills. The little information that is available on the behavior of the MSW under load indicates that the stress-strain curve can be roughly approximated by a hyperbola in which the shear stress increases at a decreasing rate as the shear strain increases. A pronounced post-peak shear strength loss is not likely to develop using this method, and a state of failure cannot easily be identified even at large strains (Jessberger and Kockel 1993).

The MSW behavior in a triaxial test is apparently controlled by the combined effect of coarse and fibre-like components of MSW, and as such, the behavior of MSW is similar to the behavior of reinforced soil systems (Jessberger and Kockel 1993). Due to the lack of information on specimen preparation, testing procedure and analysis of test data, these triaxial test results were not utilized in the current study.

Based on the range of shear strength parameters reported in the literature and the typical stress-strain response of highly organic soils, the set of stress-strain curves shown in Figure 2 was assumed to represent the MSW behavior for the purpose of this study. This stress-strain data gives the following MSW shear strength parameter values: $c_r = 12$ kPa and $\phi_r = 30^\circ$. The derivation of these values is explained in Section 4.3.1.

To the writers' knowledge, no constitutive model has been developed to represent stress-strain and shear strength behavior of MSW. Also, it has not been established to what degree the constitutive models developed for soils can be applied to MSW. For the purpose of this study, the stress-strain response of the MSW was modeled using a hyperbolic model originally developed by Duncan et al. (1980) and later modified by Seed and Duncan (1983). The model assumes that the stress-strain response follows a hyperbolic variation as given below:

$$(\sigma_1 - \sigma_3) = \frac{\varepsilon}{\frac{1}{E_t} + \frac{\varepsilon}{(\sigma_1 - \sigma_3)_u}} \quad (6)$$

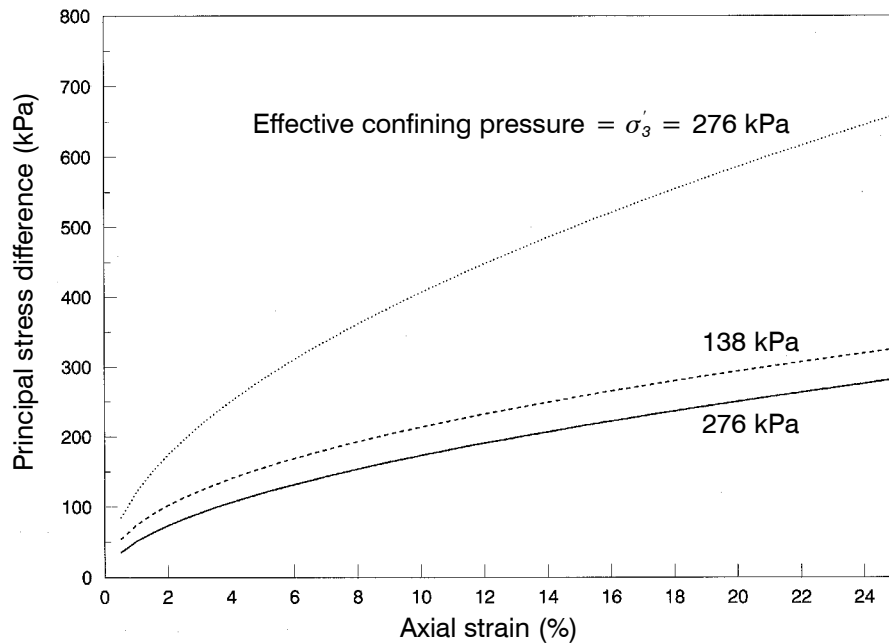


Figure 2. Stress-strain behavior of MSW.

where: $(\sigma_1 - \sigma_3)$ = principal stress difference; ε = axial strain; $(\sigma_1 - \sigma_3)_u$ = ultimate principal stress difference; and E_t = tangent Young's modulus. E_t is expressed as:

$$E_t = \left[1 - \frac{R_f(1 - \sin \phi)}{2c \cos \phi + 2\sigma'_3 \sin \phi} (\sigma_1 - \sigma_3) \right]^2 KP_a \left(\frac{\sigma'_3}{P_a} \right)^n \quad (7)$$

where: c = cohesion; and σ'_3 = effective confining pressure. For unloading-reloading, the tangent Young's modulus is denoted by E_{ur} and is expressed as:

$$E_{ur} = K_{ur} P_a \left(\frac{\sigma'_3}{P_a} \right)^n \quad (8)$$

In this hyperbolic model, the bulk modulus, B , is required and is defined as follows:

$$B = K_B P_a \left(\frac{\sigma'_3}{P_a} \right)^m \quad (9)$$

In Equations 7, 8 and 9, K , (modulus number), K_{ur} (unloading-reloading modulus number), K_B (bulk modulus number), n , m (bulk modulus exponent) and R_f are material properties. These parameters must be determined in accordance with the procedure described by Duncan et al. (1980) using the stress-strain data. The determination of these parameters for MSW based on the data in Figure 2 is described in Section 4.3.

conditions in each soil element at the beginning of the increment; and the second analysis was based on the average stress experienced during the increment.

The critical base and side slope composite liner interfaces were represented by interface elements capable of modeling a nonlinear shear response. The interface elements were zero-thickness elements made up of two parallel nodal links. The geomembrane liner was assumed to be placed on a rigid foundation material and was not allowed to deform laterally under horizontal shear stresses transmitted along the geomembrane-geotextile interface.

A typical finite element discretization used to simulate the incremental MSW loading landfill conditions is shown in Figure 4. A base length of 122 m was selected for the MSW. It was assumed that the MSW was placed in eight lifts to reach the final height of 30.5 m. The finite element analysis was also performed for the same landfill configuration but with four lifts to reach the same final height. When the number of lifts was increased from four to eight, the displacements in the base and side slope composite liner increased by approximately 2 to 9% for the smooth and textured HDPE geomembrane interfaces. Hence, eight layers of MSW was considered an optimum number of layers for these analyses.

4.2 Modeling of Landfill Composite Liner Interfaces

4.2.1 General

In the finite element analyses, the interface shear stress/shear displacement behavior was modeled using the hyperbolic zero-thickness interface model developed by Clough and Duncan (1969). Nodal links at each end of the element consisted of a normal spring (with normal stiffness K_n) and a shear spring (with tangent shear stiffness K_{st}). The normal stiffness, K_n , was assigned a very large value to avoid overlapping of the interface elements. The tangent shear stiffness, K_{st} , is given by Equations 3 and 4. The parameters required for the application of Equations 3 and 4 can be determined based on the direct shear test results. A detailed description of the procedure to calculate the model parameters is provided below and values are summarized in Table 2.

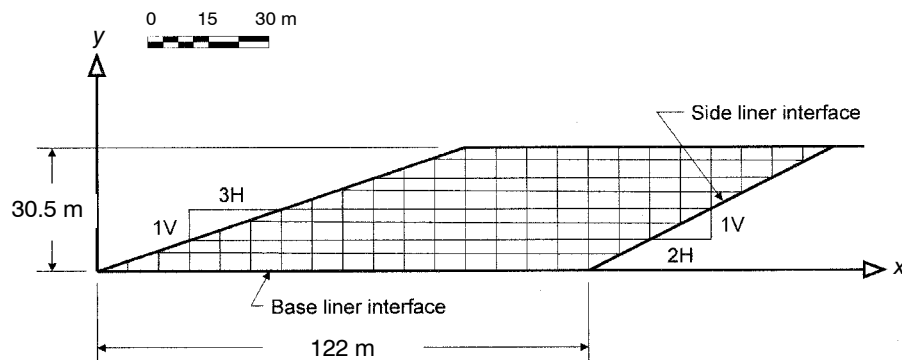


Figure 4. Finite element discretization of MSW fill.

Table 2. Summary of the hyperbolic interface model parameters.

Parameter	Smooth HDPE geomembrane- nonwoven geotextile	Textured HDPE geomembrane- nonwoven geotextile
K_s	1490	818
n	1.0	0.8
K_{ur}	1490	818
c_l	1.4 kPa	12 kPa
δ_l	11°	30°
R_f	0.9	0.9
K_n	10 ⁴	10 ⁴

4.2.2 Determination of Parameters c_l and δ_l

Based on the direct shear test data, the shear stress at failure under different normal stresses for smooth and textured HDPE geomembrane-nonwoven geotextile surfaces was determined, and plotted against normal stress. A best-fit straight line was then drawn as shown in Figure 5. The slope of this line is equal to δ_l and the intercept value is equal to c_l .

4.2.3 Determination of Parameters K_s , n and K_{ur}

The initial tangent slopes of the interface shear stress/shear displacement curves were determined. The values of K_s/γ_w and σ_n/P_a were plotted using logarithmic (log-log) axes as shown in Figure 6. The slope of the best-fit line gives the value of n , and the intercept of the line gives the value of K_s . For unloading-reloading, K_{ur} was assumed to be equal to K_s , and n_{ur} equal to n (where n_{ur} equals the unloading-reloading modulus number).

4.2.4 Parameter K_n

A value of 10,000 was assumed for K_n to ensure that no overlapping of the adjacent materials forming the interface occurred during the analyses. In comparison to many interfaces encountered in geomechanics problems, a geomembrane-geotextile interface undergoes negligibly small out-of-plane deformations. Hence, a large value of K_n is required to prevent out-of-plane behavior of the interfaces during the analyses.

4.2.5 Determination of Parameter R_f

Shear stress at failure, τ_f , was calculated based on peak shear stress from direct shear test data. To determine the ultimate shear stress, τ_{ult} , the direct shear test data was plotted using displacement, δ_s , on the x -axis and δ_s/τ on the y -axis. A best-fit straight line was then drawn. The reciprocal of the slope of the line is equal to τ_{ult} . This procedure was repeated for different normal stress values. The failure ratio, R_f , is defined as τ_f/τ_{ult} . An average R_f value of 0.9 was chosen as the most representative value for both types of interfaces considered.

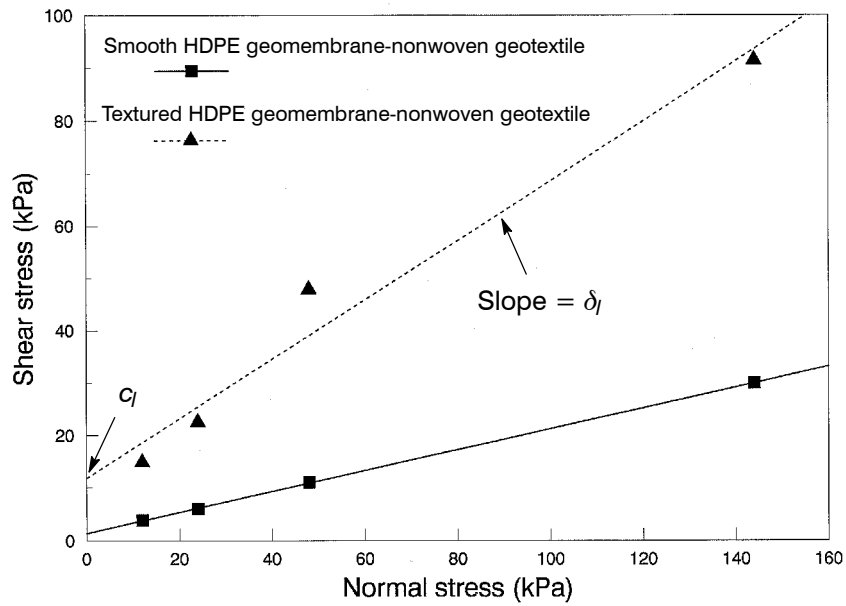


Figure 5. Determination of interface strength parameters (c_l and δ_l) for smooth and textured HDPE-nonwoven geotextile surfaces.

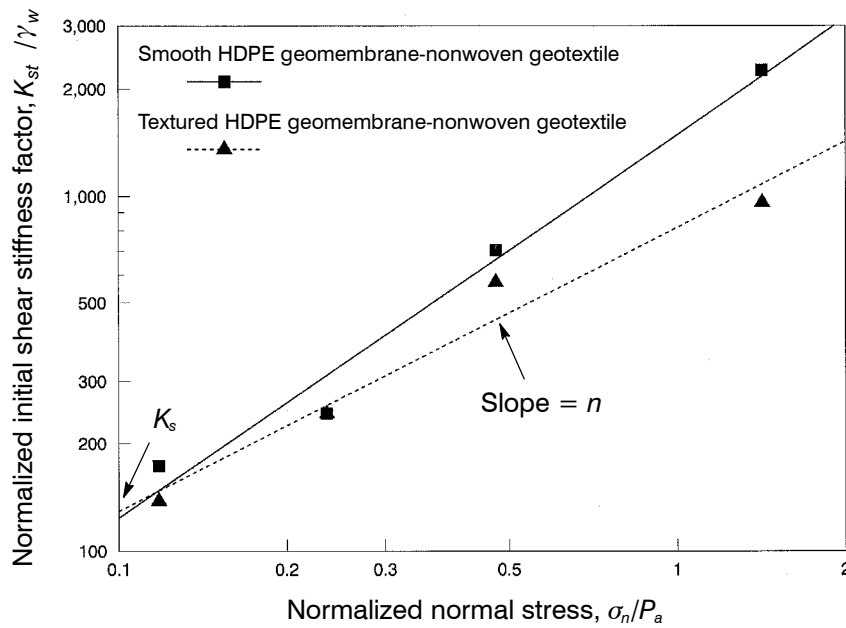


Figure 6. Determination of hyperbolic interface model parameters, K_s and n for smooth and textured HDPE-nonwoven geotextile surfaces.

4.3 Stress-Strain Model for MSW

As previously indicated, a set of stress-strain curves was assumed for the MSW (Figure 2) based on the typical behavior of organic clays and the range of strength parameters for MSW reported in the literature. The stress-strain response was modeled using a hyperbolic model. This model required determination of the parameters K , K_{ur} , K_B , n , m and R_f . The procedure used to determine these parameters is described below and values are summarized in Table 3.

4.3.1 Determination of Parameters c_r and ϕ_r

The principal stress difference at failure for different confining stresses was determined from triaxial test stress-strain curves. The Mohr-Coulomb strength envelope was constructed and the cohesion, c_r , and the friction angle, ϕ_r , for MSW determined. Using the curves in Figure 2 and the principal stress difference at 20% strain, the cohesion and internal friction angle values for the MSW were found to be 12 kPa and 30° , respectively (Figure 7).

4.3.2 Determination of Parameters K , n , K_B , m and K_{ur}

Based on the initial stress-strain data for MSW, the value of initial tangent modulus, E_i , was determined for each confining stress. The normalized confining stress (σ'_3/P_a) and normalized initial tangent modulus (E_i/P_a) were then calculated. These values were plotted on log-log axes as shown in Figure 8. The slope of the best-fit straight line gives the value of n , and the intercept of the line gives the value of K . Three values of the modulus number, $K = 100, 250$ and 400 , were assumed for the MSW. The terms “soft”, “intermediate” and “stiff” were used to identify these three conditions.

4.3.3 Determination of Parameter R_f

Stress-strain curves for the MSW were used to plot, ε versus $\varepsilon/(\sigma_1 - \sigma_3)$ for different confining stresses. A best-fit straight line was drawn. The reciprocal values of the slopes

Table 3. Summary of the calculated hyperbolic model parameters for MSW.

Parameter	Value
Cohesion, c_r	12 kPa
Friction angle, ϕ_r	30°
Failure ratio, R_f	0.9
Modulus number, K	250
Modulus number, K_{ur}	350
Modulus exponent, n	0.3
Bulk modulus number, K_B	200
Bulk modulus exponent, m	0.2

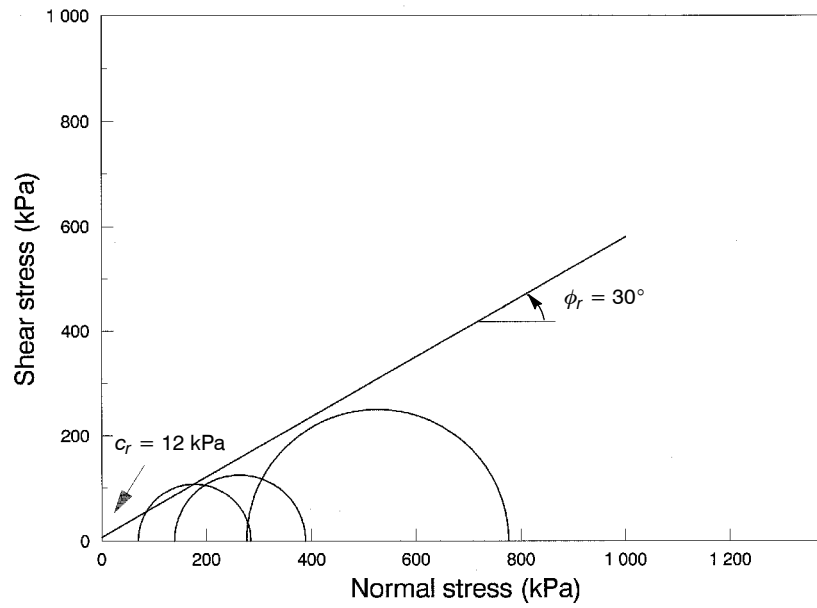


Figure 7. Determination of shear strength parameters for MSW.

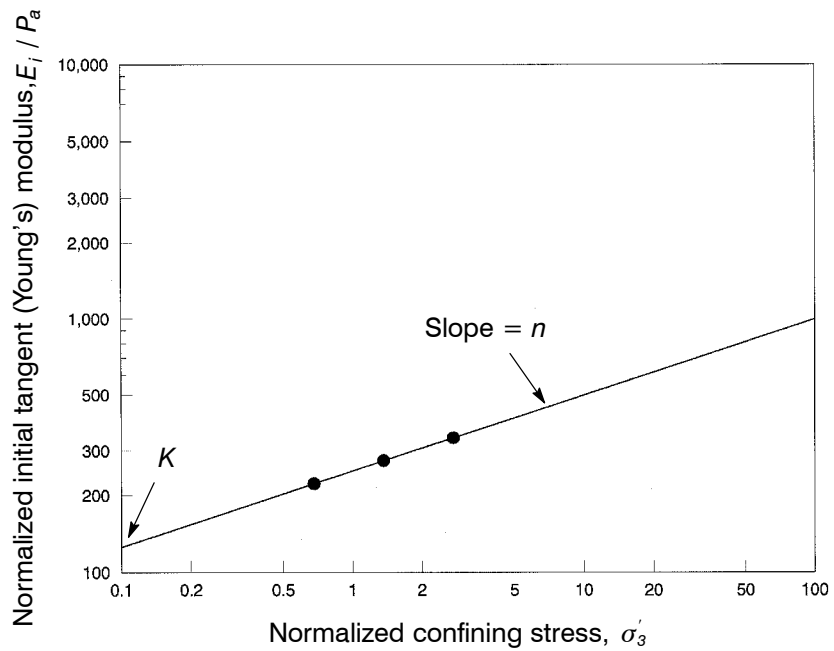


Figure 8. Determination of the hyperbolic model parameters for MSW.

of the best-fit lines gives the ultimate principal stress difference, $(\sigma_1 - \sigma_3)_u$, at each confining pressure. Knowing the principal stress difference at failure, $(\sigma_1 - \sigma_3)_f$, R_f was calculated using the relation $(\sigma_1 - \sigma_3)_f / (\sigma_1 - \sigma_3)_u$. An average value of 0.9 was chosen for the failure ratio for all analyses performed in this study.

5 RESULTS AND DISCUSSION

The numerical results obtained include the induced shear stresses and shear displacements along the two types of geosynthetic landfill composite liner interfaces after placement of each layer of MSW. These analyses also show the effects of the MSW stiffness on the interface shear stress/shear displacement behavior of geosynthetic composite liner interfaces.

5.1 Shear Stress Distribution Along the Landfill Composite Liner System

Figure 9a shows the typical variation of the interface shear stress along a smooth HDPE geomembrane-nonwoven geotextile interface for an intermediate MSW stiffness condition as the MSW height was increased from 3.8 to 30.5 m. These results are for a composite liner configuration with a side slope of 1V:2H. It can be seen that the interface shear stress generally increased as the height of the MSW increased. The shear stress along the base increased from very small values at the toe of the MSW slope to a maximum value at a point near the vertical projection of the top of the MSW slope. As the MSW thickness increased, the location of the maximum shear stress shifted laterally toward the side slope, roughly following the direction in which the top of the MSW slope moves. Beyond this point, a significant drop in the shear stress followed.

The shear stress distribution for the textured geomembrane-geotextile interface is presented in Figure 9b. The shape of the shear stress distribution diagram is approximately the same as that for the smooth geomembrane-geotextile. The maximum shear stress along the base liner for the textured geomembrane-geotextile interface was slightly less than that for the smooth geomembrane-geotextile interface. The maximum shear stress along the side slope liner for the textured geomembrane-geotextile interface was slightly more than that for the smooth geomembrane-geotextile interface. A stiffer geomembrane-geotextile interface did not appear to have a significant effect on the shear stress distribution along the composite liner interface.

5.2 Shear Displacement Distribution Along the Landfill Composite Liner System

The computed shear displacements along the landfill base and side slope for an intermediate MSW stiffness condition and a landfill side slope of 1V:2H for the smooth and textured HDPE geomembrane-nonwoven geotextile are plotted in Figures 10a and 10b. The magnitude of the shear displacements varied in a manner similar to the shear stress diagrams (Figures 9a and 9b). Along the base liner, larger shear displacements occurred beneath the MSW face slope. The shear displacements along the side slope were concentrated in an area near the base of the slope. This effect was pronounced for the textured geomembrane-geotextile interface. The displacements of the textured geomem-

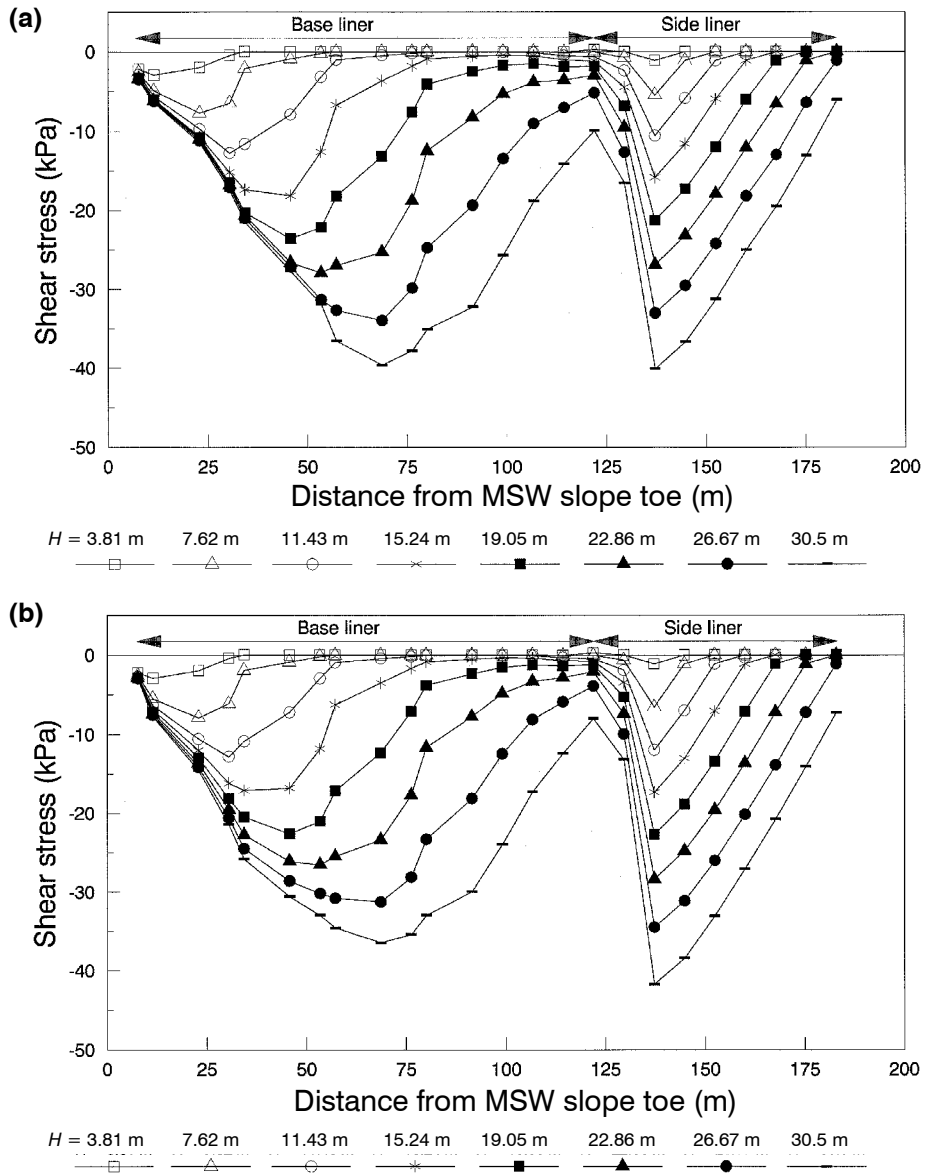


Figure 9. Shear stress distribution in base and side slope landfill composite liner for: (a) smooth HDPE geomembrane-nonwoven geotextile; (b) textured HDPE geomembrane-nonwoven geotextile.

Notes: Landfill base length = 122 m; side slope = 1V:2H; intermediate MSW stiffness condition.

brane-geotextile interface were significantly lower than those for smooth geomembrane-geotextile interface (Table 4).

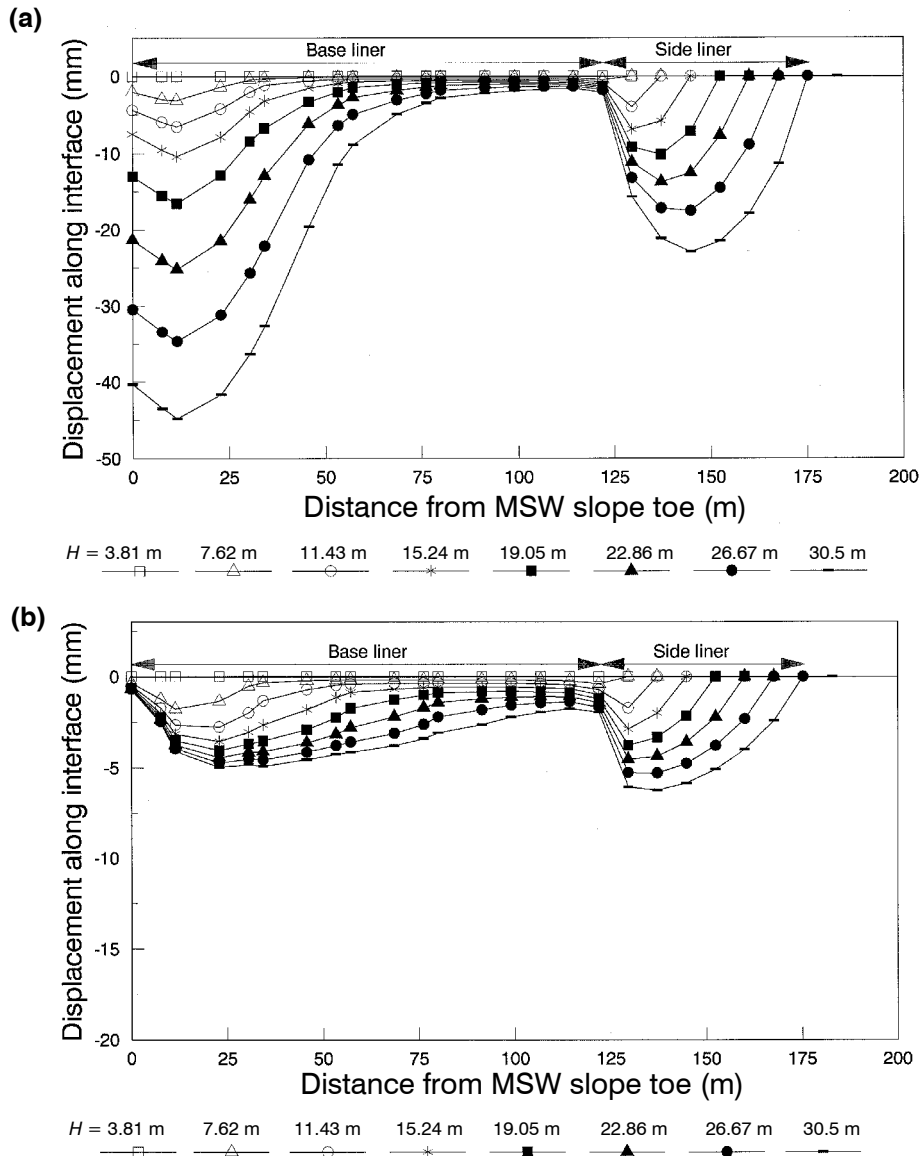


Figure 10. Landfill composite liner displacement distribution for: (a) smooth HDPE geomembrane-nonwoven geotextile; (b) textured HDPE geomembrane-nonwoven geotextile.

Notes: Landfill base length = 122 m; side slope = 1V:2H; intermediate MSW stiffness condition.

Had the critical interface been located beneath the geomembrane liner and had a interface shear stress/shear displacement behavior similar to that of the geomembrane-geotextile

Table 4. Summary of finite element analysis results.*

Landfill composite liner interface	Side liner slope	MSW condition	Maximum shear stress (kPa)		Maximum displacement (mm)	
			Side liner	Base liner	Side liner	Base liner
1.5 mm smooth HDPE geomembrane-nonwoven geotextile	1V:2H	Soft	29.4	50.3	4.0	170.9
		Intermediate	40.1	39.6	22.9	44.8
		Stiff	42.6	33.4	35.2	15.3
1.5 mm textured HDPE geomembrane-nonwoven geotextile	1V:2H	Soft	28.7	44.9	3.1	6.7
		Intermediate	41.7	36.4	6.1	4.9
		Stiff	47.7	32.0	8.6	4.1

Notes: *See Figure 3 for MSW geometry: height = 30.5 m; slope = 1V:3H; and base length = 122 m.

interface been used for this interface, then the calculated interface displacements shown in Figure 10 would generally apply to this critical interface. The tensile stiffness of the geomembrane liner is usually too small to affect the shear displacement distribution along this interface. Therefore, the displacements shown in Figure 10 should enable one to approximately evaluate the geomembrane liner tensile strains for the critical interface located immediately below the geomembrane liner. With this assumption, and for the case shown in Figure 10, the maximum tensile strain in the smooth geomembrane liner was approximately 0.3% in the base liner and 0.11% in the side liner; whereas, the corresponding values for the textured geomembrane liner were 0.008 and 0.023%, respectively. These results indicate that the tensile strains within the base geomembrane liner were generally small. Tensile strains along the side slope geomembrane liner, however, can lead to accumulated geomembrane displacements near the toe causing concerns about possible folding of the geomembrane liner.

5.3 Shear Strength Mobilization Along Landfill Composite Liner Interfaces

The relative displacements at interfaces between geosynthetics in landfill composite liners were dependent upon the level of the shear stress distribution relative to the peak shear strength of the interface. The nonlinear shear behavior of most interfaces plays a modifying role in this distribution. Figures 11a and 11b illustrate the shear stress distribution relative to the peak shear strength available along both base and side slope composite liners for smooth and textured HDPE geomembrane-nonwoven geotextile interfaces for a side slope of 1V:2H, an intermediate MSW stiffness condition, and a MSW height of 30.5 m. The available peak shear strength in each case was obtained using Equation 1.

It is evident that, for a smooth geomembrane-geotextile interface, the peak shear strength was reached over a considerable distance beneath the MSW face slope. Large portions of the side slope were also close to the failure condition. At these locations, the shear strength and shear stress curves either coincided with each other or were very close to each other. In contrast, the textured geomembrane-geotextile interface induced

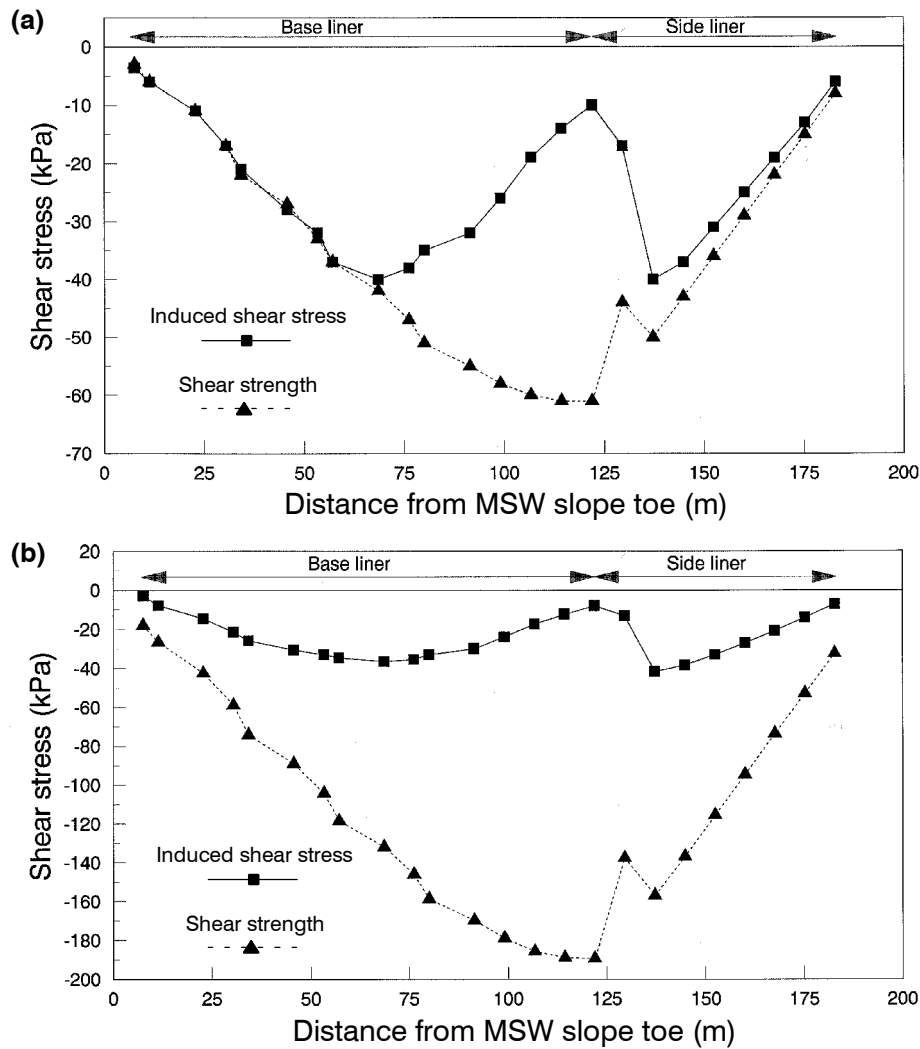


Figure 11. Mobilization of shear strength for: (a) smooth HDPE geomembrane-nonwoven geotextile; (b) textured HDPE geomembrane-nonwoven geotextile.

Notes: Landfill base length = 122 m; side slope = 1V:2H; MSW height = 30.5 m; intermediate MSW stiffness condition.

shear stress curve was considerably below the shear strength curve. This indicates a large factor of safety at all locations along the base and side slope liner in the latter case.

Since the overall factor of safety of the system based on a limit equilibrium approach was greater than 1.0, the geomembrane liner displacements along the base and side slope were largely independent of each other. Low shear displacements within the base composite liner system for a length of approximately 61 m effectively isolated the two larger displacement zones and provided increased stability.

5.4 Effect of Height of MSW on the Landfill Composite Liner Behavior

Figure 12 shows the maximum side liner displacement for smooth and textured HDPE geomembrane-geotextile interfaces with an incremental increase in MSW height for three different side slopes, 1V:2H, 1V:2.5H and 1V:3H, and intermediate MSW stiffness conditions. It was observed that placement of MSW up to a height of 7.6 m produced no displacement in the side slope composite liner system. As the height of the MSW increased, displacements increased in an approximately linear manner. For the textured geomembrane-geotextile interface, the steepness of the side slope did not appear to significantly influence the side liner displacements.

The effect of incremental loading on the maximum base liner displacement is shown in Figure 13. The displacement increased with the placement of each MSW layer, and the magnitude of base liner displacements was larger than the side slope liner displacements. The steepness of the side slope did not influence the base liner displacements.

Figures 14 and 15 show the effect of incremental loading on the maximum shear stress in the side slope liner and base liner for both the smooth and textured geomembrane-geotextile interfaces, respectively. The maximum shear stress increased linearly with increasing MSW height, and was not significantly influenced by the type of composite liner interface considered.

5.5 Effect of MSW Stiffness on the Landfill Composite Behavior

A series of parametric analyses was performed to evaluate the effects of MSW stiffness and the results are summarized below, as well as in Table 4. Table 4 shows maxi-

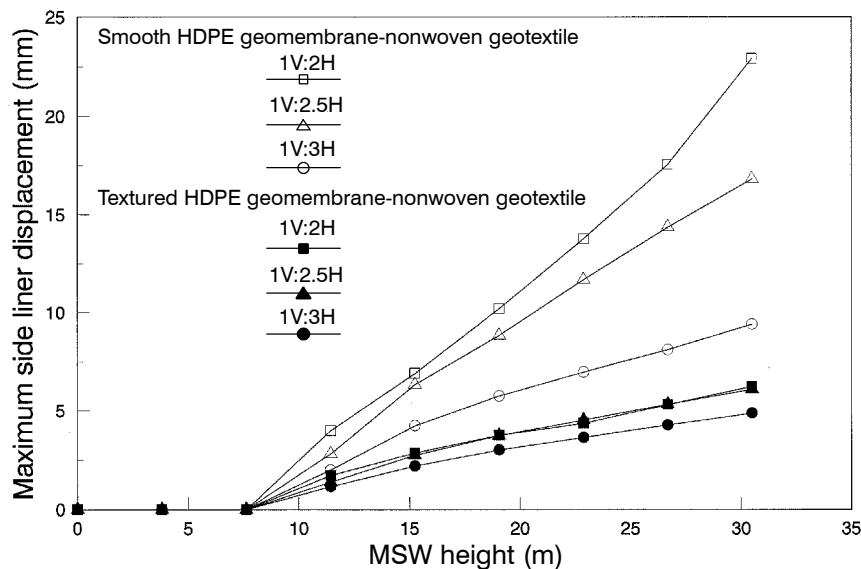


Figure 12. Effect of incremental MSW loading on maximum side slope liner displacement.

Notes: Landfill base length = 122 m; intermediate MSW stiffness condition.

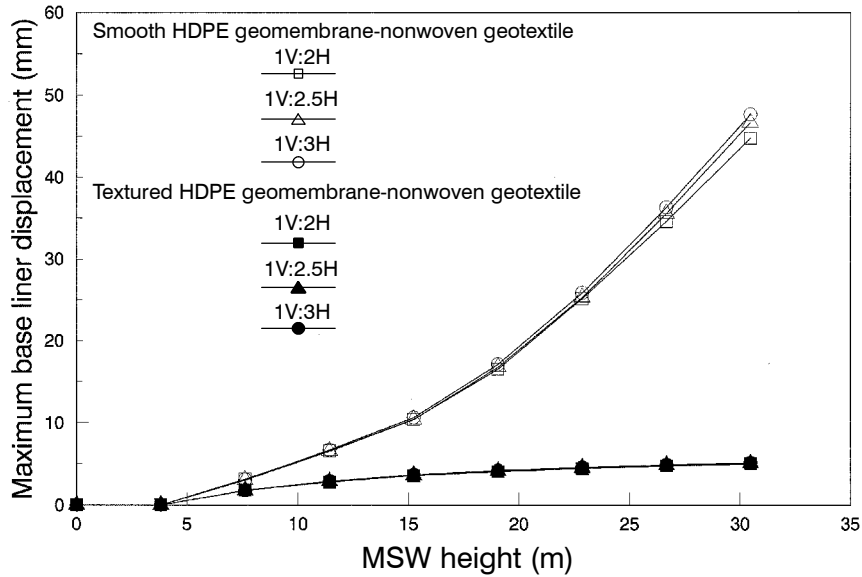


Figure 13. Effect of incremental MSW loading on maximum base liner displacement.
 Notes: Landfill base length = 122 m; intermediate MSW stiffness condition.

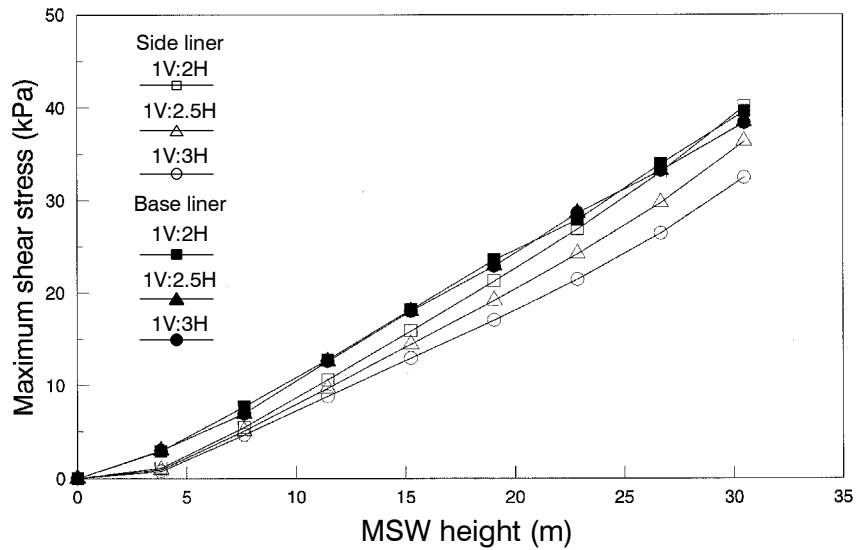


Figure 14. Effects of incremental MSW loading on maximum shear stress in smooth HDPE geomembrane-nonwoven geotextile.
 Notes: Landfill base length = 122 m; intermediate MSW stiffness condition.

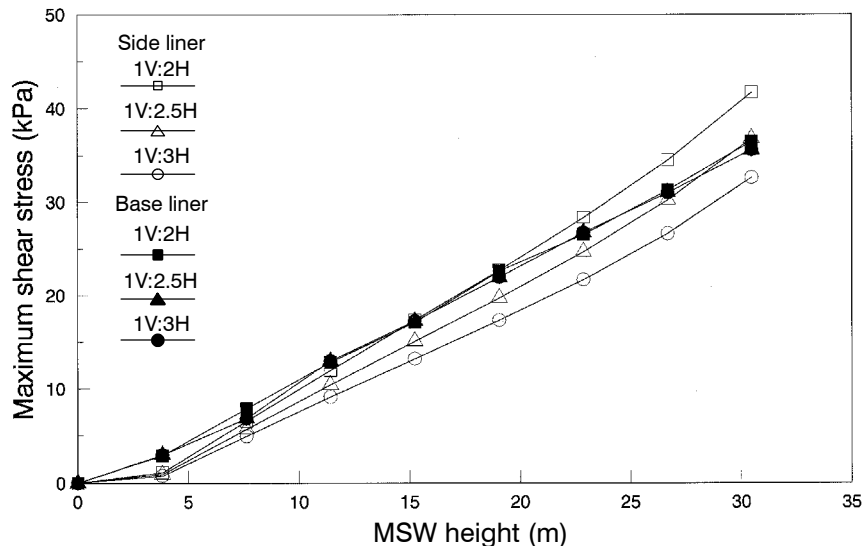


Figure 15. Effect of incremental MSW loading on maximum shear stress for a textured HDPE geomembrane-nonwoven geotextile.

Notes: Landfill base length = 122 m; intermediate MSW stiffness condition.

imum shear stress induced in the smooth geomembrane-geotextile interface along both the base and side slope liner for soft, intermediate and stiff MSW conditions. It can be seen from Table 4 that the maximum shear stress along the base liner decreased by approximately 34% when the MSW stiffness changed from soft to stiff conditions. With the increase in the MSW stiffness, the maximum shear stress along the side slope liner increased by approximately 31% from soft to stiff MSW conditions. This shear stress distribution can be explained by the fact that for the same density conditions in soft and stiff MSW, the soft MSW located within the triangular volume above the side slope liner applied a larger lateral pressure on the MSW mass located on the base liner. This resulted in an increase in the shear stresses along the base liner interface. Since the overall factor of safety along the combined base and side slope composite liner systems was the same regardless of the stiffness of the MSW, higher interface shear stresses occurred along the side liner system as MSW stiffness increased. Therefore, as the MSW stiffness increased, there was a gradual transfer of shear stress from the base to the side slope portion of the liner system. The same effect of MSW stiffness can be seen for the shear stress in the base and side slope liners (Table 4) for the textured geomembrane-geotextile interface.

The MSW stiffness condition affected the composite liner interface displacement values significantly especially for the smooth geomembrane-geotextile interface. From Table 4, it can be seen that there was a very significant decrease in the maximum base liner displacement from 170.9 mm for soft MSW to 15.3 mm for stiff MSW. The increase in the side slope liner was from 4.0 mm for soft MSW to 35.2 mm for stiff MSW. In the case of the textured geomembrane-geotextile interface, as shown in Table 4, the decrease in the maximum base liner displacement from a soft to stiff MSW condition

was approximately 41%. The corresponding increase was approximately 64% for the side slope liner displacement.

5.6 Comparison with Limit Equilibrium Analyses

Two-dimensional slope stability analyses were performed to obtain the factors of safety against sliding of the MSW block for both smooth and textured HDPE geomembrane liner interfaces. The analyses were performed using the computer code PCSTABL4 developed at Purdue University (Lovell et al. 1983). The program uses the method of slices to analyze the slope and calculates the factor of safety according to the simplified Janbu method for non-circular surfaces or Bishop's method for circular failures. The critical failure surface was specified as passing along the base and side slope liner interfaces.

The analyses were performed for both the smooth and textured geomembrane-geotextile interfaces, and used the side slope configurations considered in the finite element analyses. The factors of safety for the smooth and textured geomembrane-geotextile interfaces are given in Table 5. The maximum side and base liner displacements were computed based on the finite element analysis and are also included in Table 5 for comparison. The limit equilibrium analysis results show that the slopes are stable; however, the relative interface displacement values are not necessarily proportional to the factors of safety.

5.7 Special Case Analysis

In order to assess the interface shear stress/shear displacement behavior of the landfill composite liner system, when the factor of safety, $FS = 1$, a finite element analysis was performed for a landfill configuration that has a $FS = 1.0$. Based on limit equilibrium analyses using PCSTABL4, a landfill configuration with a side slope of 1V:2H and base length of 91.5 m resulted in $FS = 1$ for a smooth geomembrane-geotextile interface. The same landfill configuration with a textured geomembrane-geotextile interface yielded $FS = 3.5$. This configuration was then used to perform a finite element analysis. Both the smooth and the textured HDPE geomembrane-nonwoven geotextile interfaces, and intermediate stiffness MSW conditions were considered in the analyses.

Table 5. Comparison of two dimensional limit equilibrium and finite element analyses results

Side slope	Smooth HDPE geomembrane-nonwoven geotextile			Textured HDPE geomembrane-nonwoven geotextile		
	FS	Maximum base liner displacement (mm)	Maximum side liner displacement (mm)	FS	Maximum base liner displacement (mm)	Maximum side liner displacement (mm)
1V:2H	1.49	44.8	22.9	4.74	4.9	6.1
1V:2.5H	1.57	46.6	16.8	5.01	5.0	5.8
1V:3H	1.66	47.5	9.4	5.3	5.1	4.9

Note: FS = factor of safety.

The interface shear stress/shear displacement distribution along the base and side slope composite liner for smooth HDPE geomembrane-nonwoven geotextile interfaces are shown in Figures 16a and 16b, respectively. The shear strength mobilization along the base and side slope composite liner system is shown in Figure 17. Although a factor of safety of one indicates an unstable condition and imminent slippage, it is seen that the increase in computed displacements within the smooth geomembrane-geotextile interface is not significant. Caution should be exercised because the accuracy of the finite element analyses depends on the accuracy of the model for the actual interface shear stress/shear displacement behavior as well as the stress-strain behavior of the MSW. Also, the assumed stiffness of the MSW influences the interface shear stress and shear displacement distribution along the composite liner interface. The difference between the two curves in Figure 17 for $FS = 1.0$ may be partly a manifestation of the lack of total compatibility between the limit equilibrium and finite element analyses. Therefore, a unique factor of safety value, such as in the limit equilibrium method, was not obtained once it was recognized that the overall behavior of the liner system was also a function of the stress-strain characteristics of the MSW.

6 SUMMARY AND CONCLUSIONS

Finite element analyses were performed to evaluate the interface shear stress/shear displacement response of two typical landfill composite liner system interfaces as MSW was placed in increments on the landfill cell base and on the side slope. The analyses provided insight into the effects of different design variables on the interface shear stress and shear displacement distribution along the composite liner interfaces. Based on the results obtained, the following conclusions can be drawn:

- (1) The composite liner interface *shear stress* distribution does not appear to be significantly affected by the interface stiffness; however, interface *shear displacements* are strongly influenced by the interface stiffness.
- (2) All other factors being constant, the stiffness of the MSW is a major factor determining the composite liner interface shear stress and shear displacement distribution. This aspect of composite liner interface behavior cannot be predicted by limit equilibrium analyses.
- (3) Base and side slope composite liners that contain smooth HDPE geomembranes may undergo significant displacements as a result of MSW filling (including MSW placement along a portion of the side slope at the same time as base placement). The magnitude of composite liner displacements along the base and side slope can be balanced by appropriately proportioning the length of the area filled along the base and side slope.
- (4) A cell filling sequence can be devised to minimize overall shear displacements of the composite liner interfaces by appropriately dimensioning the length of MSW along the base relative to the MSW thickness. This can be achieved by placing a long enough separation along the base between the maximum shear stress zone and the toe of the side slope. This aspect of composite liner interface behavior cannot be fully evaluated by the limit equilibrium approach.

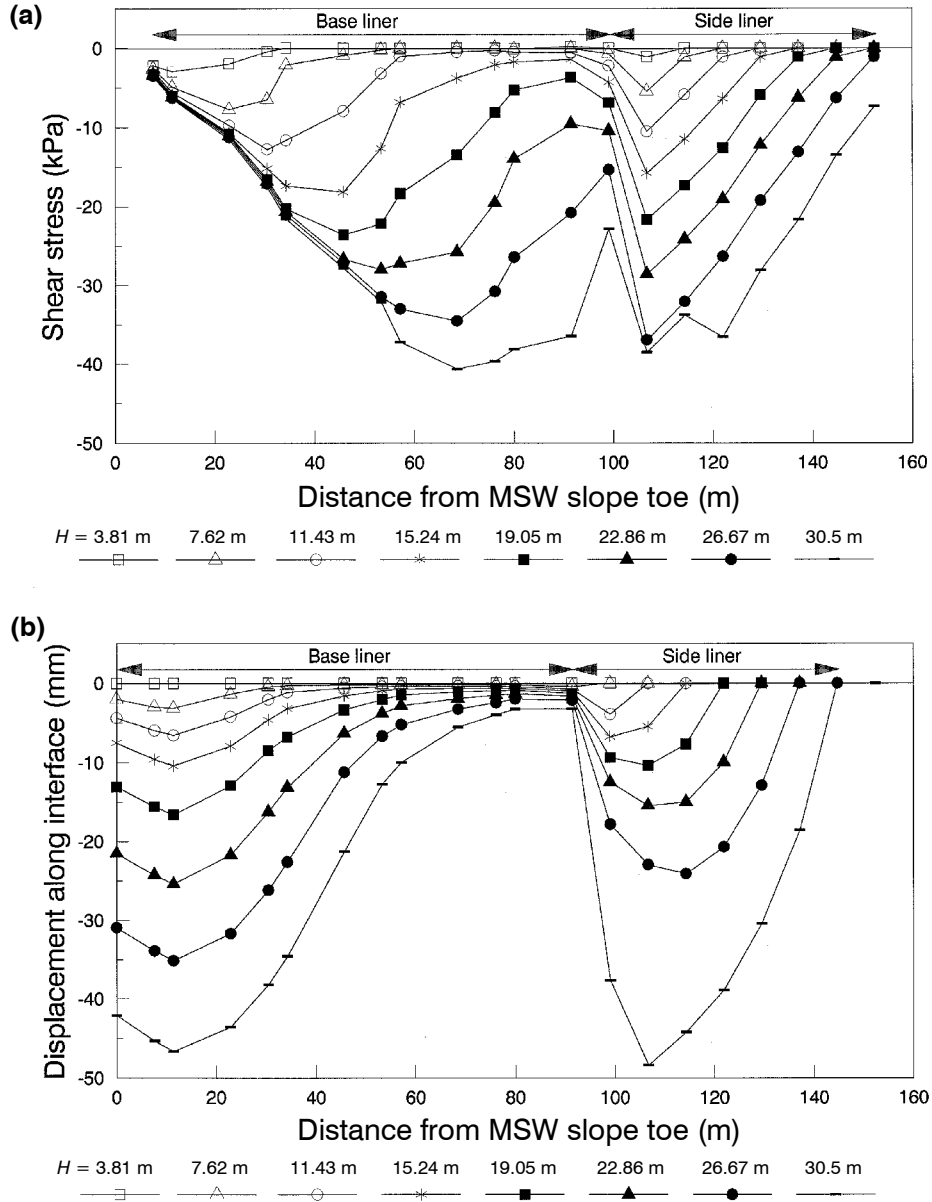


Figure 16. Smooth HDPE geomembrane-nonwoven geotextile in a landfill configuration with $FS = 1$ based on limit equilibrium analysis: (a) shear stress versus distance from MSW slope toe; (b) liner displacement distribution in base and side slope liner versus distance from MSW slope toe.

Notes: Landfill base length = 91.44 m; side slope = 1V:2H; intermediate MSW stiffness condition.

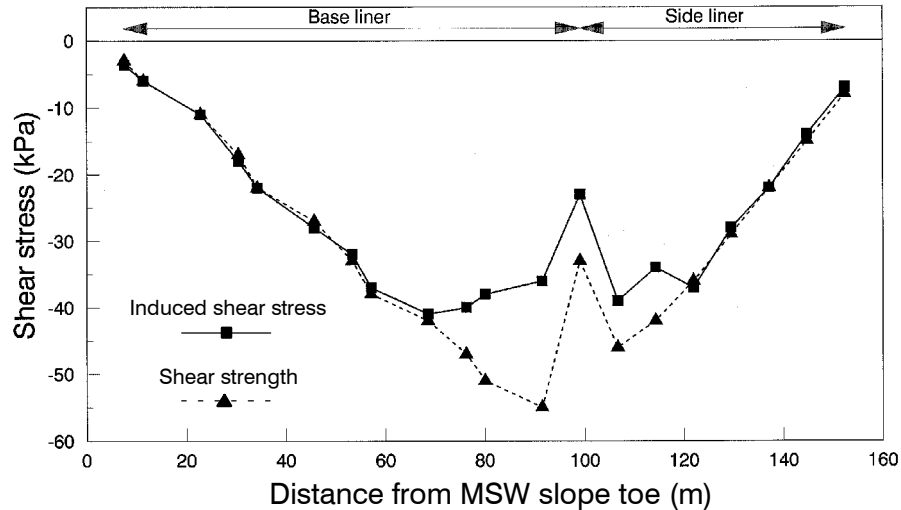


Figure 17. Mobilization of shear strength in a smooth HDPE geomembrane-nonwoven geotextile for a landfill configuration with $FS = 1$ based on limit equilibrium analysis.

Notes: Landfill base length = 91.44 m; side slope = 1V:2H; MSW height = 30.5 m; intermediate MSW stiffness condition.

- (5) An increase in the side slope from 1V:3H to 1V:2H can produce a significant increase in side slope composite liner displacement, particularly for smooth geomembrane liner interfaces. Use of flatter side slopes can prevent excessive composite liner interface displacements, but also reduces the available airspace for MSW disposal.
- (6) While finite element method analyses provide a valuable tool to evaluate the composite liner interface stresses and displacements, successful application of this procedure depends on the correct use of stress-strain parameters representing composite liner materials and interface behavior. In general, strength and compressibility characteristics of MSW are not well understood and need further evaluation.

Additionally, the analyses provided evidence that, if the critical plane is located beneath the geomembrane liner, the following conclusions may be drawn:

- (7) The maximum tensile strain in the geomembrane liner under typical filling conditions is likely to be significantly lower than the yield strain of commonly used geomembrane landfill liners. However, MSW depths greater than 30.5 m were not considered in this study, and thus require further evaluation.
- (8) The build-up of composite liner interface shear displacements along the side slope can lead to significant wrinkling or folding of the geomembrane liner near the base of the slope. This is particularly important when smooth geomembranes are used. This aspect of composite liner interface behavior cannot be revealed by limit equilibrium analyses.

- (9) The smooth HDPE geomembrane-nonwoven geotextile interfaces beneath interior MSW face slopes reached the peak shear strength condition. The mechanism that prevents composite liner failure in such cases is the internal strength of the landfill MSW.

REFERENCES

- ASTMD 5321, "Test Method for Determining the Coefficient of Soil and Geosynthetics or Geosynthetic and Geosynthetic Friction by the Direct Shear Method", American Society for Testing and Materials, West Conshohocken, Pennsylvania, USA.
- Boulanger, R.W., Bray, J.D., Chew, S.H., Seed, R.B., Mitchell, J.K. and Duncan, J.M., 1991, "SSCOMPPC: A Finite Element Analysis Program for Evaluation of Soil-Structure Interaction and Compaction Effects", Report No. UCB/GT/91-02, University of California, Berkeley, California, USA, 176 p.
- Byrne, R.J., Kendall, J. and Brown, S., 1992, "Cause and Mechanism of Failure, Kettleman Hills Landfill B-19, Unit IA", *Stability and Performance of Slopes and Embankments-II*, Seed, R.B. and Boulanger, R.W., Editors, Geotechnical Special Publication No. 31, ASCE, 1992, proceedings of a specialty conference held in Berkeley, California, USA, Vol. 2, pp. 1188-1215.
- Clough, G.W. and Duncan, J.M., 1969, "Finite Element Analyses of Port Allen and Old River Locks", Report Number TE 69-3, University of California, Berkeley, California, USA, 264 p.
- Duncan, J.M., 1992, "State-of-the-Art: Static Stability and Deformation Analysis", *Stability and Performance of Slopes and Embankments-II*, Seed, R.B. and Boulanger, R.W., Editors, Geotechnical Special Publication No. 31, ASCE, 1992, proceedings of a specialty conference held in Berkeley, California, USA, Vol. 1, pp. 222-266.
- Duncan, J.M., Byrne, P., Wong, K.S. and Mabry, P., 1980, "Strength, Stress-Strain and Bulk Modulus Parameters for Finite Element Analyses of Stresses and Movements in Soil Masses", Report Number UCB/GT/80-01, University of California, Berkeley, California, USA, 70 p.
- Fang, H.Y., Slutter, R.J. and Koerner, R.M., 1977, "Load Bearing Capacity of Compacted Waste Materials", *Proceedings of the Ninth International Conference on Soil Mechanics and Foundation Engineering*, Specialty Session on Geotechnical Engineering and Environmental Control, Vol. 4, Tokyo, Japan, July 1977, pp. 265-278.
- Jessberger, H.L. and Kockel, R., 1993, "Mechanische Eigenschaften von Siedlungsabfall-Labor- und Modellversuche", *Geotechnische Probleme beim Bau Von Abfalldeponien 9*, Nurnberger Deponieseminar, pp. 1-24.
- Koerner, R.M., 1994, "Designing with Geosynthetics", 3rd Edition, Prentice Hall, Englewood Cliffs, New Jersey, USA, 783 p.
- Kosgi, S. and Reddy, K.R., 1995, "Deformation Characteristics of Landfill Composite Liners Under Incremental Refuse Loading Conditions", Report Number UIC-GGEL-95-04, University of Illinois at Chicago, Chicago, Illinois, USA, 116 p.

- Landva, A.O. and Clark, J.I., 1990, "Geotechnics of Waste Fills," *Geotechnics of Waste Landfills - Theory and Practice*, Landva, A. and Knowles, G.D., Editors, ASTM Special Publication 1070, proceedings of a symposium held in Pittsburgh, Pennsylvania, USA, pp. 86-108.
- Lovell, C.W., Sharma, S. and Carpenter, J.R., 1983, "*Introduction to Slope Stability Analysis with STABLA*", Report prepared for Federal Highway Administration, U.S. Department of Transportation, 109 p.
- Martin, R.B., Koerner, R.M. and Whitty, J.E., 1984, "Experimental Friction Evaluation of Slippage Between Geomembranes, Geotextiles and Soils", *Proceedings of the International Conference on Geomembranes*, IFAI, Denver, Colorado, USA, June 1984, pp. 191-196.
- Mitchell, J.K., Seed, R.B. and Seed, H.B., 1990, "Kettleman Hills Waste Landfill Slope Failure. I: Liner System Properties", *Journal of Geotechnical Engineering*, Vol. 116, No. 4, pp. 647-668.
- Mitchell, R.A. and Mitchell, J.K., 1992, "Stability Evaluation of Waste Landfills", *Stability and Performance of Slopes and Embankments-II*, Seed, R.B. and Boulanger, R.W., Editors, Geotechnical Special Publication No. 31, ASCE, 1992, proceedings of a specialty conference held in Berkeley, California, USA, Vol. 2, pp.1152-1187.
- Poran, C.J. and Ali, F.A., 1989, "Properties of Solid Waste Incinerator Fly Ash", *Journal of Geotechnical Engineering*, Vol. 115, No. 5, pp. 1118-1133.
- Seed, R.B. and Duncan, J.M., 1983, "*Soil Structure Interaction Effects of Compaction-Induced Stresses and Deflections*", Report Number UCB/GT/83-06, University of California, Berkeley, California, USA, 425 p.
- Sharma, H.D. and Lewis, S.P., 1994, "*Waste Containment Systems, Waste Stabilization, and Landfills: Design and Evaluation*", John Wiley and Sons, Inc., New York, New York, USA, 588 p.
- Seed, R.B., Mitchell, J.K. and Seed, H.B., 1990, "Kettleman Hills Waste Landfill Slope Failure. I: Liner System Properties", *Journal of Geotechnical Engineering*, Vol. 116, No. 4, pp. 669-690.
- Siegel, R.A., Robertson, R.J. and Anderson, D.G., 1990, "Slope Stability Investigations at a Landfill in Southern California", *Geotechnics of Waste Landfills - Theory and Practice*, Landva, A. and Knowles, G.D., Editors, ASTM Special Publication 1070, proceedings of a symposium held in Pittsburgh, Pennsylvania, USA, pp. 259-284.
- Singh, S. and Murphy, B., 1990, "Evaluation of the Stability of Sanitary Landfills", *Geotechnics of Waste Landfills - Theory and Practice*, Landva, A. and Knowles, G.D., Editors, ASTM Special Publication 1070, proceedings of a symposium held in Pittsburgh, Pennsylvania, USA, pp. 240-258.
- Tchobanoglous, G., Theisen, H. and Vigil, S., 1993, "*Integrated Solid Waste Management: Engineering Principles and Management Issues*", McGraw-Hill, Inc., New York, New York, USA, 978 p.

NOTATIONS

Basic SI units are given in parentheses.

B	=	bulk modulus (N/m^2)
c	=	cohesion (N/m^2)
c_l	=	adhesion between interface materials (N/m^2)
c_r	=	cohesion of MSW (N/m^2)
E_t	=	tangent Young's modulus (N/m^2)
E_{ur}	=	unloading-reloading tangent Young's modulus (N/m^2)
K	=	modulus number (dimensionless)
K_B	=	bulk modulus number (dimensionless)
K_{Jur}	=	unloading-reloading shear coefficient (dimensionless)
K_n	=	normal spring stiffness in finite element analysis (N/m^3)
K_s	=	shear coefficient (dimensionless)
K_{st}	=	tangent shear stiffness (N/m^3)
K_{ur}	=	unloading-reloading modulus number (dimensionless)
m	=	bulk modulus exponent (dimensionless)
n	=	modulus exponent (dimensionless)
n_{ur}	=	unloading-reloading modulus exponent (dimensionless)
P_a	=	atmospheric pressure (N/m^2)
R_f	=	failure ratio (dimensionless)
δ_l	=	interface friction angle of geosynthetic landfill composite liner components ($^\circ$)
δ_s	=	average relative shear displacement (m)
γ_w	=	unit weight of water (N/m^3)
ε	=	axial strain (dimensionless)
σ_n	=	effective normal stress on the shear plane (N/m^2)
σ_3'	=	effective confining pressure (N/m^2)
$\sigma_1 - \sigma_3$	=	principal stress difference (N/m^2)
$(\sigma_1 - \sigma_3)_f$	=	principal stress difference at failure (N/m^2)
$(\sigma_1 - \sigma_3)_u$	=	ultimate principal stress difference (N/m^2)
τ	=	shear stress (N/m^2)
τ_f	=	shear stress at failure (N/m^2)
τ_p	=	interface shear strength between two materials (N/m^2)
τ_{ult}	=	ultimate shear stress (N/m^2)
ϕ	=	internal friction angle ($^\circ$)
ϕ_r	=	internal friction angle of MSW ($^\circ$)